Performance of density functionals for computation of core electron binding energies in first-row hydrides and glycine

ARTICLE *in* THEORETICAL CHEMISTRY ACCOUNTS · MARCH 2014

Impact Factor: 2.23 · DOI: 10.1007/s00214-014-1473-x

2 AUTHORS, INCLUDING:

Iogann Tolbatov
Notre Dame Radiation Laboratory
13 PUBLICATIONS **7** CITATIONS

Theor Chem Acc (2014) 133:1473
DOI 10.1007/s00214-014-1473-x

REGULAR ARTICLE

Performance of density functionals for computation of core electron binding energies in first-row hydrides and glycine

Iogann Tolbatov · Daniel M. Chipman

Received: 14 February 2014 / Accepted: 21 February 2014

Abstract A number of density functionals are benchmarked for calculation of 1s core electron binding energies for carbon, nitrogen, and oxygen nuclei in glycine, and for comparison in the first-row hydrides methane, ammonia, and water. The goal is to establish methods having potential to aid the analysis of experimental X-ray photoelectron spectra on compounds such as amino acids, DNA nucleosides, and large polypeptides in various environments. Several promising density functionals are identified that can reproduce experimental results within 0.2 eV on average for the absolute binding energies and also for the intramolecular and intermolecular shifts in the studied molecules.

Keywords Quantum chemistry · Density functional theory · Core electron binding energies · X-ray photoelectron spectroscopy · Glycine

Dedicated to the memory of Professor Isaiah Shavitt and published as part of the special collection of articles celebrating his many contributions.

Electronic supplementary material The online version of this article (doi:10.1007/s00214-014-1473-x) contains supplementary material, which is available to authorized users.

I. Tolbatov · D. M. Chipman (✉)
Notre Dame Radiation Laboratory, University of Notre Dame, Notre Dame, IN 46556, USA
e-mail: chipman.1@nd.edu

I. Tolbatov
Department of Physics, University of Notre Dame, Notre Dame, IN 46556, USA

1 Introduction

Biomolecules on metal surfaces are being widely studied for their practical applicability in areas such as biosensors [1–5], organic semiconductors [6–10], and biocatalysis [11–15]. X-ray photoelectron spectroscopy is a valuable nondestructive tool in this area of research, as recently demonstrated by its use to characterize the adsorption of thymidine [16], histidine [17], and histidine tripeptide [17] on gold and copper surfaces. To facilitate the interpretation of such photoelectron spectra, we have initiated a project to establish accurate and efficient methods for computation of core electron binding energies (CEBEs) in amino acids, DNA nucleotides, and polypeptides. As a first step, the present paper benchmarks the performance of various density functional methods for calculation of carbon, nitrogen, and oxygen CEBEs in the model compound glycine, and for comparison also in the first-row hydrides methane, ammonia, and water.

Glycine is the smallest of the 21 amino acids that form proteins [18]. It plays an essential role in living animals [19, 20] and plants [21, 22] and has even been found in space [23, 24] advocating the idea of panspermia. Its main function in animals is to serve as a building block for protein formation. Previous analyses of glycine in the gas phase include several experimental investigations [25–27]. A computational [28] investigation of gas phase glycine based on density functional theory showed an average absolute deviation from the experimental [25] CEBEs of just 0.2 eV, though the particular method used was later declared obsolete because it depended on a fortuitous cancelation of errors [29]. Shifts in the glycine CEBEs from the gas phase have also been studied in neutral, acidic, and basic solutions by means of X-ray photoelectron spectroscopy and by theoretical methods [30].

Published online: 25 March 2014

High accuracy in CEBE calculations can be reliably achieved with ab initio post-Hartree–Fock methods. For example, it was shown recently that the observed shifts of carbon 1s photoelectron energies in some organic compounds could be reproduced on average to within 0.03 eV by means of Møller–Plesset many-body perturbation theory and coupled cluster approaches [31]. However, such high accuracy methods are generally too expensive to be applied to large molecules.

The most promising approaches for efficient electronic structure calculations on large molecules are generally based on density functional theory with Kohn–Sham orbitals [32–35]. The most efficient such method for CEBEs is based on Koopmans' theorem, but this approach has quite limited accuracy [36–39]. Better accuracy can be obtained from calculations based on an effective core potential [40–45], an equivalent core approximation [46–48], a fractionally occupied transition state [49–52], or with a ΔSCF approach [29, 31, 53–57]. Time-dependent density functional theory is also widely used for CEBE calculation [58–62], wherein the best results are usually given with functionals having a long-range correction [63, 64].

A study using the ΔSCF approach for CEBEs of first-row atoms in many small gas phase molecules found that the quality of the results was very sensitive to the choice of functional [29], with the best performance found corresponding to a mean unsigned error (MUE) from experiment of just 0.16 eV. Similar accuracy was also found for the first-row atoms in gas phase thymine [65, 66].

In the present study, we use the ΔSCF approach with Hartree–Fock and a wide variety of pure and hybrid density functional approaches to study CEBEs in glycine, methane, ammonia, and water. Each approach is evaluated for its accuracy in reproducing experimental values for the absolute CEBEs in all four molecules, as well as for the intramolecular and intermolecular chemical shifts between like nuclei in the same or different molecules. Several promising candidates are found that can be recommended for future testing to establish accurate and efficient methods for calculations of CEBEs and their chemical shifts in large biomolecules.

2 Computational methods

Separate initial state and final core–hole state calculations provided ΔSCF values of the CEBEs. The maximum overlap method [67, 68] was used to prevent variational collapse of the final hole state. This simply replaces the usual aufbau criterion for occupying orbitals in each iteration with a criterion that the occupied orbitals be selected to overlap as much as possible with those of the previous iteration. The Ahlrichs' VTZ basis set [69] was used, based on the very good results it provided in a recent MCSCF-MRPT study of CEBEs in simple hydrides [39]. All calculations were performed with the Q-Chem 4.0 program [70, 71].

Hartree–Fock (HF) and a variety of exchange, correlation, and hybrid functionals were considered in this study. The local spin density approximation is represented by the exchange functional S (Slater and Dirac 1930) [72] together with the correlation functionals VWN (Vosko, Wilk, and Nusair) [73], PZ81 (Perdew and Zunger) [74], and PW92 (Perdew and Wang 1992) [75].

Generalized gradient approximation (GGA) functionals examined in this work include the exchange functionals B (Becke 1988) [76] and PW91 (Perdew and Wang 1991) [77, 78], together with the correlation functionals PW91 (Perdew and Wang 1991) [77, 78], P86 (Perdew 1986) [79], and LYP (Lee, Yang, and Parr) [80]. The correlation part of PBE (Perdew, Burke, and Ernzerhof 1996) [81] was used as well in the schemes PBEOP (PBE exchange with the reparametrized one-parameter progressive correlation functional) [82] and PBE0 (PBE hybrid with 25 % HF exchange) [83]. Other hybrid schemes considered were B97 [84], B97-1 [85], B97-2 [86] (a family of Becke 1997 hybrids), BOP (Becke 1988 with the OP correlation functional) [82], B3PW91 [87], B3LYP [88], and B3LYP5 [73, 76]. In addition, the empirical density functional EDF1 [89] was utilized.

Meta-GGA functionals incorporate the Laplacian of the electron density and generally depend on the electron kinetic energy density. These features allow a systematic improvement of results for many quantum chemical calculations. We have used the exchange functional BR89 (Becke-Roussel 1989 represented in analytic form) [87, 90] and the correlation functional B94 (Becke 1994) [90, 91]. Minnesota functionals tested are M05 [92], M05-2X [93], M06-L [94], M06-HF [95], M06 [96], M06-2X [96], and M11 [97]. Another global hybrid studied is BMK [98]. A hybrid extension of the nonempirical exchange–correlation TPSS (Tao, Perdew, Staroverov, and Scuseria) [99] and functional TPSSh [100] is also examined.

Several range-corrected and asymptotically corrected schemes have been studied as well. The long-range-corrected functionals considered include μBOP [101] (a long-range-corrected version of BOP) and the hybrids ωB97 and ωB97X [102]. The asymptotically corrected exchange–correlation potential considered is LB94, which is a linear combination of an LDA exchange–correlation potential and the LB (van Leeuwen and Baerends) [103] exchange potential. Short-range-corrected functionals that were specifically formulated for the treatment of core-excited states include SRC1 and SRC2 [104], which we have implemented with the BLYP functional and a recommended set of parameters for designing the shape of the long-range and short-range Hartree–Fock components (SRC1: $C_{\mathrm{SHF}} = 0.50$, $\mu_{\mathrm{SR}} = 0.56\ a_0^{-1}$, $C_{\mathrm{LHF}} = 0.17$, $\mu_{\mathrm{LR}} = 2.45\ a_0^{-1}$;

Table 1 Experimental values for CEBEs of C, N, and O nuclei in CH_4, NH_3, H_2O, and glycine

Molecule	Orbital	Binding energy measured (eV)	Experimental references [25, 105–108]
CH_4	C 1s	290.83	Nordfors et al. [105]
			Pireaux et al. [106]
NH_3	N 1s	405.60	Jolly et al. [107]
H_2O	O 1s	539.91	Nordfors et al. [108]
glycine	C (methyl carbon) 1s	292.25	Slaughter et al. [25]
	C (carboxyl carbon) 1s	295.15	
	N 1s	405.58	
	O (keto oxygen) 1s	538.2	
	O (hydroxyl oxygen) 1s	540.0	

Table 2 Experimental values for chemical shifts

Chemical shift	Experimental value (eV)
$\Delta E^C\left(\mathrm{Gly}_{\mathrm{methyl}\,C}, \mathrm{Gly}_{\mathrm{carboxyl}\,C}\right)$	−2.90
$\Delta E^O(\mathrm{Gly}_{\mathrm{keto}\,O}, \mathrm{Gly}_{\mathrm{hydroxyl}\,O})$	−1.75
$\Delta E^C\left(\mathrm{CH_4}, \mathrm{Gly}_{\mathrm{methyl}\,C}\right)$	1.42
$\Delta E^C\left(\mathrm{CH_4}, \mathrm{Gly}_{\mathrm{carboxyl}\,C}\right)$	4.32
$\Delta E^N(\mathrm{NH_3}, \mathrm{Gly}_N)$	−0.02
$\Delta E^O(\mathrm{H_2O}, \mathrm{Gly}_{\mathrm{keto}\,O})$	−1.71
$\Delta E^O\left(\mathrm{H_2O}, \mathrm{Gly}_{\mathrm{hydroxyl}\,O}\right)$	0.09

SRC2: $C_{\mathrm{SHF}} = 0.55$, $\mu_{\mathrm{SR}} = 0.69\ a_0^{-1}$, $C_{\mathrm{LHF}} = 0.08$, $\mu_{\mathrm{LR}} = 1.02\ a_0^{-1}$) [104].

For purposes of discussion, the various functionals considered are separated into seven categories, those being HF, LSDA, GGA, hybrid GGA, meta-GGA, meta-GGA hybrid, and range or asymptotically corrected functionals. Results from a larger collection that further includes some possible combinations that are mixed between the categories, for instance exchange LSDA + correlation GGA, exchange GGA + correlation meta-GGA, etc., were also calculated. Those mixed category results generally turned out to be less promising and so are relegated to the Electronic Supplementary Material, where details of the molecular geometries used are also documented.

3 Results and discussion

Table 1 lists experimentally measured values of the eight absolute CEBEs under consideration, those being the three carbon nuclei in methane and the methyl and carboxyl carbons in glycine, the two nitrogen nuclei in ammonia and glycine, and the three oxygen nuclei in water and the keto and hydroxyl oxygens in glycine. Table 2 shows the seven experimental values for the following intermolecular and intramolecular chemical shifts between like nuclei.

Table 3 MUE values in eV for CEBEs and chemical shifts computed by HF and various density functionals

Type of DFT functional	Density functional	MUE for	
		CEBEs	Chemical shifts
HF	HF	0.37	0.59
LSDA	SPW92	3.84	0.26
	SPZ81	3.76	0.26
	SVWN	3.83	0.26
GGA	BOP	0.12	0.17
	BLYP	0.27	0.16
	BP86	0.17	0.18
	BPBE	0.35	0.19
	BPW91	0.16	0.19
	EDF1	0.32	0.17
	PBEOP	0.12	0.17
	PW91LYP	0.24	0.16
	PW91P86	0.15	0.19
	PW91PBE	0.38	0.19
	PW91PW91	0.19	0.18
Hybrid GGA	B3LYP	0.46	0.26
	B3LYP5	0.35	0.26
	B3PW91	0.15	0.27
	B97	0.51	0.25
	B97-1	0.68	0.27
	B97-2	0.23	0.27
	PBE0	0.20	0.30
Meta-GGA	BR89B94	0.55	0.24
	M06L	0.11	0.19
Meta-GGA hybrid	BMK	2.04	0.35
	M05	0.24	0.30
	M052X	0.88	0.47
	M06	0.26	0.32
	M062X	0.26	0.42
	M06HF	0.45	0.61
	M11	0.92	0.94
	TPSSh	0.31	0.18
Range or asymptotically corrected	BLYP-SRC1	1.32	0.99
	BLYP-SRC2	3.93	0.37
	LB94	20.05	5.65
	μBOP	0.52	0.35
	ωB97	0.60	0.35
	ωB97X	0.73	0.35

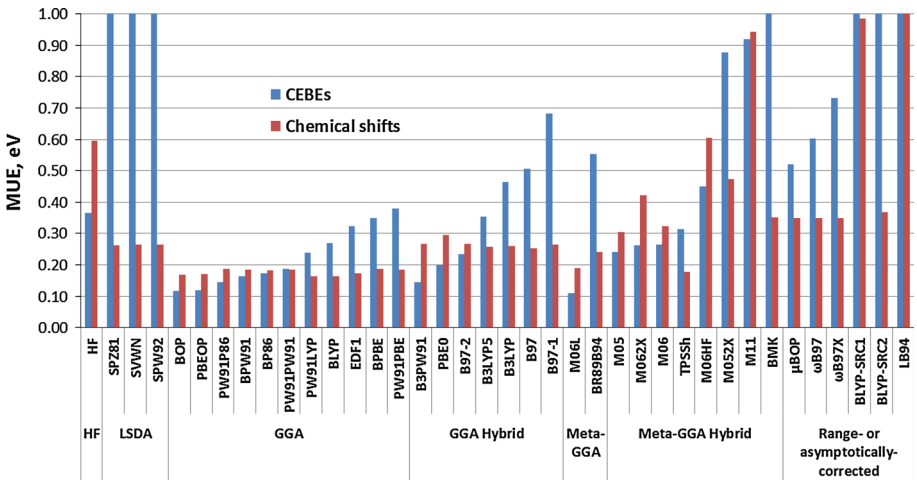

Fig. 1 MUE values for calculated CEBEs and chemical shifts

Intermolecular chemical shifts

$$\Delta E^{C}(\mathrm{CH_4}, \mathrm{Gly}_{\mathrm{methyl}\,C}) = BE(C\,1\mathrm{s}\,\mathrm{in}\,\mathrm{CH_4}) - BE(\mathrm{methyl}\,C\,1\mathrm{s}\,\mathrm{in}\,\mathrm{glycine}) \quad (1)$$

$$\Delta E^{C}(\mathrm{CH_4}, \mathrm{Gly}_{\mathrm{carboxyl}\,C}) = BE(C\,1\mathrm{s}\,\mathrm{in}\,\mathrm{CH_4}) - BE(\mathrm{carboxyl}\,C\,1\mathrm{s}\,\mathrm{in}\,\mathrm{glycine}) \quad (2)$$

$$\Delta E^{N}(\mathrm{NH_3}, \mathrm{Gly}_{N}) = BE(N\,1\mathrm{s}\,\mathrm{in}\,\mathrm{NH_3}) - BE(N\,1\mathrm{s}\,\mathrm{in}\,\mathrm{glycine}) \quad (3)$$

$$\Delta E^{O}(\mathrm{H_2O}, \mathrm{Gly}_{\mathrm{keto}\,O}) = BE(O\,1\mathrm{s}\,\mathrm{in}\,\mathrm{H_2O}) - BE(\mathrm{keto}\,O\,1\mathrm{s}\,\mathrm{in}\,\mathrm{glycine}) \quad (4)$$

$$\Delta E^{O}(\mathrm{H_2O}, \mathrm{Gly}_{\mathrm{hydroxyl}\,O}) = BE(O\,1\mathrm{s}\,\mathrm{in}\,\mathrm{H_2O}) - BE(\mathrm{hydroxyl}\,O\,1\mathrm{s}\,\mathrm{in}\,\mathrm{glycine}) \quad (5)$$

Intramolecular chemical shifts

$$\Delta E^{C}(\mathrm{Gly}_{\mathrm{methyl}\,C}, \mathrm{Gly}_{\mathrm{carboxyl}\,C}) = BE(\mathrm{methyl}\,C\,1\mathrm{s}\,\mathrm{in}\,\mathrm{glycine}) - BE(\mathrm{carboxyl}\,C\,1\mathrm{s}\,\mathrm{in}\,\mathrm{glycine}) \quad (6)$$

$$\Delta E^{O}(\mathrm{Gly}_{\mathrm{keto}\,O}, \mathrm{Gly}_{\mathrm{hydroxyl}\,O}) = BE(\mathrm{keto}\,O\,1\mathrm{s}\,\mathrm{in}\,\mathrm{glycine}) - BE(\mathrm{hydroxyl}\,O\,1\mathrm{s}\,\mathrm{in}\,\mathrm{glycine}) \quad (7)$$

Table 3 shows the MUEs from experiment for various computational methods. A full listing of the computed CEBEs and chemical shifts for each computational method is given in the Electronic Supplementary Material. The MUE results are also shown graphically in Fig. 1, which is cut off at 1 eV because methods having errors larger than that are of little interest. The functionals in Fig. 1 are ordered primarily according to the category and within each category according to the accuracy of the CEBE calculation.

HF treatment gives only modest accuracy for the CEBEs, with a MUE of 0.37 eV, and even less accuracy for the chemical shifts, with a MUE of 0.59 eV. The LSDA functionals' performance is not very good either, with very large MUEs of almost 4 eV for the CEBEs, although the chemical shifts are given fairly well with MUE of 0.26 eV.

The GGA category of functionals performs best overall. The BOP and PBEOP hybrids yield very good MUEs of 0.12 eV for CEBEs and 0.17 eV for chemical shifts. The BP86, BPW91, PW91P86, and PW91PW91 functionals also all yield MUEs of less than 0.20 eV for both CEBEs and chemical shifts. While the remaining GGA functionals have MUEs of 0.24 eV or more for the CEBEs, the errors are systematic enough to cancel somewhat in the chemical shifts, giving MUEs below 0.20 eV in all cases.

Among the hybrid GGAs, B3PW91 and PBE0 have MUEs of 0.20 eV or less for CEBEs, but these two along with all the other hybrid GGAs have somewhat higher MUEs of 0.25–0.30 eV for the chemical shifts.

The meta-GGA functional M06L performs very well, with MUEs of 0.11 eV for CEBES and 0.19 eV for chemical shifts, while the BR89B94 functional gives a high MUE of 0.55 eV for the CEBEs.

None of the meta-GGA hybrids perform consistently well, with MUEs for CEBEs all being 0.24 eV or more and MUEs for chemical shifts all being 0.30 eV or more.

Perhaps surprisingly, the range-corrected methods perform poorly, with MUEs of 0.52 eV or more for CEBEs and 0.35 eV or more for chemical shifts, and the asymptotically corrected LB94 functional performs very poorly for both CEBEs and chemical shifts.

Unsurprisingly, we can conclude that a functional's good performance in the calculation of CEBEs almost necessarily means a good description of chemical shifts, but the converse is not true.

4 Conclusion

A variety of pure and hybrid functionals has been studied for ΔSCF calculation of CEBEs and chemical shifts of C, N, and O nuclei in the first-row hydrides and glycine. Seven functionals are found that perform consistently well, giving MUEs of less than 0.20 eV for both CEBEs and chemical shifts. These are the GGA functionals BOP, PBEOP, PW91P86, BPW91, BP86, and PW91PW91 and the meta-GGA functional M06L. These can all be recommended for further study to identify suitable candidates for the interpretation of photoelectron spectra of large biomolecules.

Acknowledgments This material is based upon work supported by the Department of Energy under Award Number DE-SC0002216. This is Contribution No. NDRL-5005 from the Notre Dame Radiation Laboratory.

References

1. Ebersole RC, Miller JA, Moran JR, Ward MD (1990) Spontaneously formed functionally active avidin monolayers on metal surfaces: a strategy for immobilizing biological reagents and design of piezoelectric biosensors. J Am Chem Soc 112:3239–3241
2. Homola J (2003) Present and future of surface plasmon resonance biosensors. Anal Bioanal Chem 377:528–539
3. Du H, Disney MD, Miller BL, Krauss TD (2003) Hybridization-based unquenching of DNA hairpins on Au surfaces: prototypical "molecular beacon" biosensors. J Am Chem Soc 125:4012–4013
4. Haes AJ, Zou S, Schatz GC, Van Duyne RP (2004) Nanoscale optical biosensor: short range distance dependence of the localized surface plasmon resonance of noble metal nanoparticles. J Phys Chem B 108:6961–6968
5. Du H, Strohsahl CM, Camera J, Miller BL, Krauss TD (2005) Sensitivity and specificity of metal surface-immobilized "molecular beacon" biosensors. J Am Chem Soc 127:7932–7940
6. Gerischer H, Heller A (1991) The role of oxygen in photooxidation of organic molecules on semiconductor particles. J Phys Chem 95:5261–5267
7. Hill I, Rajagopal A, Kahn A, Hu Y (1998) Molecular level alignment at organic semiconductor-metal interfaces. Appl Phys Lett 73:662–664
8. Hamers RJ, Coulter SK, Ellison MD, Hovis JS, Padowitz DF, Schwartz MP, Greenlief CM, Russell JN (2000) Cycloaddition chemistry of organic molecules with semiconductor surfaces. Acc Chem Res 33:617–624
9. Gao Y (2010) Surface analytical studies of interfaces in organic semiconductor devices. Mater Sci Eng R-Rep 68:39–87
10. Lee WH, Park J, Sim SH, Lim S, Kim KS, Hong BH, Cho K (2011) Surface—directed molecular assembly of pentacene on monolayer graphene for high-performance organic transistors. J Am Chem Soc 133:4447–4454
11. Zayats M, Pogorelova SP, Kharitonov AB, Lioubashevski O, Katz E, Willner I (2003) Au nanoparticle-enhanced surface plasmon resonance sensing of biocatalytic transformations. Chem Eur J 9:6108–6114
12. Wu L, Payne GF (2004) Biofabrication: using biological materials and biocatalysts to construct nanostructured assemblies trends. Biotechnol 22:593–599
13. Willner I, Baron R, Willner B (2006) Growing metal nanoparticles by enzymes. Adv Mater 18:1109–1120
14. Mahapatro A, Johnson DM, Patel DN, Feldman MD, Ayon AA, Agrawal CM (2006) Surface modification of functional self–assembled monolayers on 316L stainless steel via lipase catalysis. Langmuir 22:901–905
15. Carley A, Davies P, Roberts M (2011) Oxygen transient states in catalytic oxidation at metal surfaces. Catal Today 169:118–124
16. Plekan O, Feyer V, Ptasińska S, Tsud N, Cháb V, Matolín V, Prince KC (2010) Photoemission study of thymidine adsorbed on Au (111) and Cu (110). J Phys Chem C 114:15036–15041
17. Feyer V, Plekan O, Ptasińska S, Iakhnenko M, Tsud N, Prince KC (2012) Adsorption of histidine and a histidine tripeptide on Au (111) and Au (110) from acidic solution. J Phys Chem C 116:22960–22966
18. Wagner I, Musso H (1983) New naturally—occurring amino-acids. Angew Chem Int Ed 22:816–828
19. Zhang Y, Li X, Peng L, Wang G, Ke K, Jiang Z (2012) Novel glycine—dependent inactivation of NMDA receptors in cultured hippocampal neurons. Neurosci Bull 28:550–560
20. Euden J, Mason SA, Viero C, Thomas NL, Williams AJ (2013) Investigations of the contribution of a putative glycine hinge to ryanodine receptor channel gating. J Biol Chem 288:16671–16679
21. McFarland JW, Ruess RW, Kielland K, Pregitzer K, Hendrick R (2010) Glycine mineralization in situ closely correlates with soil carbon availability across six North American forest ecosystems. Biogeochemistry 99:175–191
22. Rothstein DE (2010) Effects of amino-acid chemistry and soil properties on the behavior of free amino acids in acidic forest soils. Soil Biol Biochem 42:1743–1750
23. Belloche A, Menten KM, Comito C, Müller HSP, Schilke P, Ott J, Thorwirth S, Hieret C (2008) Detection of amino acetonitrile in Sgr B2(N). Astron Astrophys 482:179–196
24. Escamilla-Roa E, Moreno F (2013) Adsorption of glycine on cometary dust grains: II-effect of amorphous water ice. Planet Space Sci 75:1–10
25. Slaughter A, Banna M (1988) Core-photoelectron binding-energies of gaseous glycine—correlation with its proton affinity and gas–phase acidity. J Phys Chem 92:2165–2167
26. Plekan O, Feyer V, Richter R, Coreno M, de Simone M, Prince KC, Carravetta V (2007) Investigation of the amino acids glycine, proline, and methionine by photoemission spectroscopy. J Phys Chem A 111:10998–11005
27. Plekan O, Feyer V, Richter R, Coreno M, de Simone M, Prince KC, Carravetta V (2007) Photoemission and the shape of amino acids. Chem Phys Lett 442:429–433
28. Chong D (1996) Density functional calculation of core-electron binding energies of glycine conformers. Can J Chem 74:1005–1007
29. Takahata Y, Chong DP (2003) DFT calculation of core-electron binding energies. J Electron Spectrosc Relat Phenom 133:69–76
30. Ottosson N, Børve KJ, Spångberg D, Bergersen H, Sæthre LJ, Faubel M, Pokapanich W, Öhrwall G, Björneholm O, Winter B (2011) On the origins of core-electron chemical shifts of small biomolecules in aqueous solution: insights from photoemission and ab initio calculations of glycine(aq). J Am Chem Soc 133:3120–3130
31. Holme A, Borve KJ, Saethre LJ, Thomas TD (2011) Accuracy of calculated chemical shifts in carbon 1s ionization energies from single-reference ab initio methods and density functional theory. J Chem Theory Comput 7:4104–4114
32. Chong DP (ed) (1995) Recent advances in density functional methods: Part I. Recent advances in computational chemistry, vol 1. World Scientific Publishing Co Pte Ltd, Singapore
33. Chong DP (ed) (1997) Recent advances in density functional methods: Part II. Recent advances in computational chemistry, vol 1. World Scientific Publishing Co Pte Ltd, Singapore

34. Maruhn J, Reinhard P, Suraud E (2010) Density functional theory. In: Simple models of many-fermion systems. Springer, Berlin, pp 143–161
35. Nalewajski RF (2012) Density functional theory. In: Perspectives in electronic structure theory. Springer, Berlin, pp 255–368
36. Inoue C, Kaneda Y, Aida M, Endo K (1995) Simulation of XPS of poly (vinyl alcohol), poly (acrylic acid), poly (vinyl acetate), and poly (methyl methacrylate) polymers by an ab initio MO method using the model molecules. Polym J 27:300–309
37. Endo K, Maeda S, Aida M (1997) Simulation of C1s spectra of C- and O- containing polymers in XPS by ab initio MO calculations using model oligomers. Polym J 29:171–181
38. Bureau C, Chong DP, Endo K, Delhalle J, Lecayon G, Le Moël A (1997) Recent advances in the practical and accurate calculation of core and valence XPS spectra of polymers: from interpretation to simulation? Nucl Instr Meth Phys Res B 131:1–12
39. Shirai S, Yamamoto S, Hyodo S (2004) Accurate calculation of core-electron binding energies: multireference perturbation treatment. J Chem Phys 121:7586–7594
40. Pettersson LG, Wahlgren U, Gropen O (1983) Effective core potential calculations using frozen orbitals applications to transition metals. Chem Phys 80:7–16
41. Panas I, Siegbahn P, Wahlgren U (1987) Model studies of the chemisorption of hydrogen and oxygen on nickel surfaces. I. The design of a one-electron effective core potential which includes 3d relaxation effects. Chem Phys 112:325–337
42. Mattsson A, Panas I, Siegbahn P, Wahlgren U, Akeby H (1987) Model studies of the chemisorption of hydrogen and oxygen on Cu (100). Phys Rev B 36:7389–7401
43. Nyberg M, Hasselström J, Karis O, Wassdahl N, Weinelt M, Nilsson A, Pettersson LG (2000) The electronic structure and surface chemistry of glycine adsorbed on Cu (110). J Chem Phys 112:5420–5427
44. Oltedal V, Borve K, Saethre L, Thomas T, Bozek J, Kukk E (2004) Carbon 1s photoelectron spectroscopy of six-membered cyclic hydrocarbons. Phys Chem Chem Phys 6:4254–4259
45. Carroll TX, Thomas TD, Sæthre LJ, Børve KJ (2009) Additivity of substituent effects core-ionization energies and substituent effects in fluoromethylbenzenes. J Phys Chem A 113:3481–3490
46. Johansson B, Mårtensson N (1980) Core-level binding-energy shifts for the metallic elements. Phys Rev B 21:4427–4457
47. Grunze M, Brundle C, Tomanek D (1982) Adsorption and decomposition of ammonia on a W (110) surface: photoemission fingerprinting and interpretation of the core level binding energies using the equivalent core approximation. Surf Sci 119:133–149
48. Plashkevych O, Privalov T, Agren H, Carravetta V, Ruud K (2000) On the validity of the equivalent cores approximation for computing X-ray photoemission and photoabsorption spectral bands. Chem Phys 260:11–28
49. Hadjisavvas N, Theophilou A (1985) Rigorous formulation of Slater's transition-state theory for excited states. Phys Rev A 32:720–724
50. Wang S, Schwarz W (1996) Simulation of nondynamical correlation in density functional calculations by the optimized fractional orbital occupation approach: application to the potential energy surfaces of O and SO. J Chem Phys 105:4641–4648
51. Triguero L, Plashkevych O, Pettersson L, Agren H (1999) Separate state vs transition state Kohn-Sham calculations of X-ray photoelectron binding energies and chemical shifts. J Electron Spectrosc Relat Phenom 104:195–207
52. Goddard JD, Orlova G (1999) Density functional theory with fractionally occupied frontier orbitals and the instabilities of the Kohn-Sham solutions for defining diradical transition states: ring-opening reactions. J Chem Phys 111:7705–7712
53. Bagus PS (1965) Self-consistent-field wave functions for hole states of some Ne-like and Ar-like ions. Phys Rev 139:A619–A634
54. Naves de Brito A, Correia N, Svensson S, Ågren HA (1991) Theoretical study of X-ray photoelectron spectra of model molecules for polymethylmethacrylate. J Chem Phys 95:2965–2974
55. Takahashi O, Pettersson LG (2004) Functional dependence of core-excitation energies. J Chem Phys 121:10339–10345
56. Myrseth V, Sæthre LJ, Børve KJ, Thomas TD (2007) The substituent effect of the methyl group carbon 1s ionization energies, proton affinities, and reactivities of the methylbenzenes. J Org Chem 72:5715–5723
57. Saethre LJ, Borve KJ, Thomas TD (2011) Chemical shifts of carbon 1s ionization energies. J Electron Spectrosc Relat Phenom 183:2–9
58. Furche F, Ahlrichs R (2002) Adiabatic time-dependent density functional methods for excited state properties. J Chem Phys 117:7433–7447
59. Stener M, Fronzoni G, De Simone M (2003) Time dependent density functional theory of core electrons excitations. Chem Phys Lett 373:115–123
60. Fronzoni G, Stener M, Decleva P, Wang F, Ziegler T, Van Lenthe E, Baerends E (2005) Spin–orbit relativistic time dependent density functional theory calculations for the description of core electron excitations: $TiCl_4$ case study. Chem Phys Lett 416:56–63
61. Rappoport D, Furche F (2005) Analytical time-dependent density functional derivative methods within the RI-J approximation, an approach to excited states of large molecules. J Chem Phys 122(064105):1–8
62. Chong DP (2005) Density functional calculation of K-shell spectra of small molecules. J Electron Spectrosc Relat Phenom 148:115–121
63. Yanai T, Tew DP, Handy NC (2004) A new hybrid exchange-correlation functional using the Coulomb-attenuating method (CAM-B3LYP). Chem Phys Lett 393:51–57
64. Besley NA, Peach MJG, Tozer DJ (2009) Time-dependent density functional theory calculations of near-edge X-ray absorption fine structure with short-range corrected functionals. Phys Chem Chem Phys 11:10350–10358
65. Takahata Y, Okamoto AK, Chong DP (2006) DFT calculation of core-electron binding energies of pyrimidine and purine bases. Int J Quantum Chem 106(13):2581–2586
66. Takahata Y, Marques ADS (2010) Accurate core-electron binding energy shifts from density functional theory. J Electron Spectrosc Relat Phenom 178:80–87
67. Gilbert ATB, Besley NA, Gill PMW (2008) Self-consistent field calculations of excited states using the maximum overlap method (MOM). J Phys Chem A 112:13164–13171
68. Hanson-Heine MWD, George MW, Besley NA (2013) Calculating excited state properties using Kohn-Sham density functional theory. J Chem Phys 138(064101):1–8
69. Schafer A, Horn H, Ahlrichs R (1992) Fully optimized contracted Gaussian-basis sets for atoms Li to Kr. J Chem Phys 97:2571–2577
70. Shao Y, Molnar LF, Jung Y, Kussmann J, Ochsenfeld C, Brown ST, Gilbert AT, Slipchenko LV, Levchenko SV, O'Neill DP et al (2006) Advances in methods and algorithms in a modern quantum chemistry program package. Phys Chem Chem Phys 8:3172–3191
71. Krylov AI, Gill PMW (2013) Q-Chem: an engine for innovation. WIREs Comput Mol Sci 3:317–326
72. Dirac P (1930) Note on exchange phenomena in the Thomas atom. Proc Cambridge Philos Soc 26:376–385
73. Vosko S, Wilk L, Nusair M (1980) Accurate spin-dependent electron liquid correlation energies for local spin-density calculations—a critical analysis. Can J Phys 58:1200–1211

74. Perdew J, Zunger A (1981) Self-interaction correction to density-functional approximations for many-electron systems. Phys Rev B 23:5048–5079
75. Perdew J, Wang Y (1992) Accurate and simple analytic representation of the electron-gas correlation-energy. Phys Rev B 45:13244–13249
76. Becke A (1988) Density-functional exchange-energy approximation with correct asymptotic-behavior. Phys Rev A 38:3098–3100
77. Perdew JP (1991) Unified theory of exchange and correlation beyond the local density approximation. In: Ziesche P, Eschrig H (eds) Electronic structure of solids' 91. Akademie-Verlag, Berlin, pp 11–20
78. Perdew JP, Wang Y (1992) Accurate and simple analytic representation of the electron-gas correlation energy. Phys Rev B 45:244–249
79. Perdew J (1986) Density-functional approximation for the correlation-energy of the inhomogeneous electron-gas. Phys Rev B 33:8822–8824
80. Lee C, Yang W, Parr R (1988) Development of the Colle-Salvetti correlation-energy formula into a functional of the electron-density. Phys Rev B 37:785–789
81. Perdew J, Burke K, Ernzerhof M (1996) Generalized gradient approximation made simple. Phys Rev Lett 77:3865–3868
82. Tsuneda T, Suzumura T, Hirao K (1999) A new one-parameter progressive Colle–Salvetti-type correlation functional. J Chem Phys 110:10664–10678
83. Adamo C, Scuseria G, Barone V (1999) Accurate excitation energies from time-dependent density functional theory: assessing the PBE0 model. J Chem Phys 111:2889–2899
84. Becke A (1997) Density-functional thermochemistry. V. Systematic optimization of exchange-correlation functionals. J Chem Phys 107:8554–8560
85. Hamprecht F, Cohen A, Tozer D, Handy N (1998) Development and assessment of new exchange-correlation functionals. J Chem Phys 109:6264–6271
86. Wilson PJ, Bradley TJ, Tozer DJ (2001) Hybrid exchange-correlation functional determined from thermochemical data and ab initio potentials. J Chem Phys 115:9233–9242
87. Becke A, Roussel M (1989) Exchange holes in inhomogeneous systems: a coordinate-space model. Phys Rev A 39:3761–3767
88. Stephens P, Devlin F, Chabalowski C, Frisch MJ (1994) Ab initio calculation of vibrational absorption and circular dichroism spectra using density functional force fields. J Phys Chem 98:11623–11627
89. Adamson RD, Gill PM, Pople JA (1998) Empirical density functionals. Chem Phys Lett 284:6–11
90. Proynov E, Gan Z, Kong J (2008) Analytical representation of the Becke-Roussel exchange functional. Chem Phys Lett 455:103–109
91. Becke A (1994) Thermochemical tests of a kinetic-energy dependent exchange-correlation approximation. Int J Quant Chem S28:625–632
92. Zhao Y, Schultz NE, Truhlar D (2005) Exchange-correlation functional with broad accuracy for metallic and nonmetallic compounds, kinetics, and noncovalent Interactions. J Chem Phys 123(161103):1–4
93. Zhao Y, Schultz N, Truhlar D (2006) Design of density functionals by combining the method of constraint satisfaction with parametrization for thermochemistry, thermochemical kinetics, and noncovalent interactions. J Chem Theory Comput 2:364–382
94. Zhao Y, Truhlar DG (2006) A new local density functional for main-group thermochemistry, transition metal bonding, thermochemical kinetics, and noncovalent interactions. J Chem Phys 125(194101):1–18
95. Zhao Y, Truhlar DG (2006) Density functional for spectroscopy: no long-range self-interaction error, good performance for Rydberg and charge-transfer states, and better performance on average than B3LYP for ground states. J Phys Chem A 110:13126–13130
96. Zhao Y, Truhlar DG (2008) The M06 suite of density functionals for main group thermochemistry, thermochemical kinetics, noncovalent interactions, excited states, and transition elements: two new functionals and systematic testing of four M06-class functionals and 12 other functionals. Theor Chem Acc 120:215–241
97. Peverati R, Truhlar DG (2011) Improving the accuracy of hybrid meta-GGA density functionals by range separation. J Phys Chem Lett 2:2810–2817
98. Boese A, Martin J (2004) Development of density functionals for thermochemical kinetics. J Chem Phys 121:3405–3416
99. Tao J, Perdew J, Staroverov V, Scuseria G (2003) Climbing the density functional ladder: nonempirical meta-generalized gradient approximation designed for molecules and solids. Phys Rev Lett 91(146401):1–4
100. Staroverov V, Scuseria G, Tao J, Perdew J (2003) Comparative assessment of a new nonempirical density functional: molecules and hydrogen-bonded complexes. J Chem Phys 119:12129–12137
101. Song J, Hirosawa T, Tsuneda T, Hirao K (2007) Long-range corrected density functional calculations of chemical reactions: redetermination of parameter. J Chem Phys 126(154105):1–7
102. Chai J, Head-Gordon M (2008) Systematic optimization of long-range corrected hybrid density functionals. J Chem Phys 128(084106):1–15
103. Van Leeuwen R, Baerends E (1994) Exchange-correlation potential with correct asymptotic behavior. Phys Rev A 49:2421–2431
104. Besley NA, Peach MJ, Tozer DJ (2009) Time-dependent density functional theory calculations of near-edge X-ray absorption fine structure with short-range corrected functionals. Phys Chem Chem Phys 11:10350–10358
105. Nordfors D, Agren H (1991) Calculation of core electron-binding energies from structural formulas. J Electron Spectrosc Relat Phenom 56:1–11
106. Pireaux J, Svensson S, Basilier E, Malmqvist P, Gelius U, Gaudano R, Siegbahn K (1976) Core-electron relaxation energies and valence-band formation of linear alkanes studied in gas-phase by means of electron-spectroscopy. Phys Rev A 14:2133–2145
107. Jolly W, Bomben K, Eyermann C (1984) Core-electron binding-energies for gaseous atoms and molecules. At Data Nucl Data Tables 31:433–493
108. Nordfors D, Nilsson A, Martensson N, Svensson S, Gelius U, Agren H (1981) X-ray excited photoelectron-spectra of free molecules containing oxygen. J Electron Spectrosc Relat Phenom 56:117–164